ELECTRONIC SUPPLEMENTARY INFORMATION FOR

Luminescent Macroporous Aerogels of Two-Dimensional Nanocrystals of Metal Halide Perovskites with Adjustable Semiconducting Bandgaps

Penghao Guo, [a] Xuelian Jiang [a] and Pei-Xi Wang *[a]

[a] i-Lab, Suzhou Institute of Nano-Tech and Nano-Bionics of the Chinese Academy of Sciences, 398 Ruoshui Road, Suzhou, Jiangsu 215123, P. R. China

*Correspondence: pxwang2020@sinano.ac.cn

EXPERIMENTAL METHODS

Materials

Lead(II) oxide (99.0 %, Sigma-Aldrich), 2-phenylethylamine (99.0 %, Sigma-Aldrich), hydrobromic acid (48 wt.% in H_2O, Sigma-Aldrich), hydroiodic acid (57 wt.% in H_2O, 99.95%, Sigma-Aldrich), manganese(II) bromide (anhydrous, 99%, Thermo Scientific Chemicals), N,N-dimethylformamide (anhydrous, 99.8%, Sigma-Aldrich), cis-1-amino-9-octadecene (oleylamine; 98 %, Aldrich), cis-9-octadecenoic acid (oleic acid; 99 %, Sigma-Aldrich), chlorobenzene (anhydrous, 99.8 %, Sigma-Aldrich), and cyclohexane (anhydrous, 99.5 %, Sigma-Aldrich) were used as received.

Characterizations

Atomic force microscopy was conducted on a Bruker Dimension Icon Atomic Force Microscope with ScanAsyst. Field emission scanning electron spectroscopy were performed on a Hitachi Regulus 8230 Ultra-high Resolution Scanning Electron Microscope. Powder X-ray diffraction patterns were collected on a Bruker D8 ADVANCE Diffractometer using copper K-alpha radiation (with a wavelength of 0.15406 nm). Photoluminescence excitation and emission spectroscopy were performed on a Hitachi F-4600 Fluorescence Spectrophotometer.

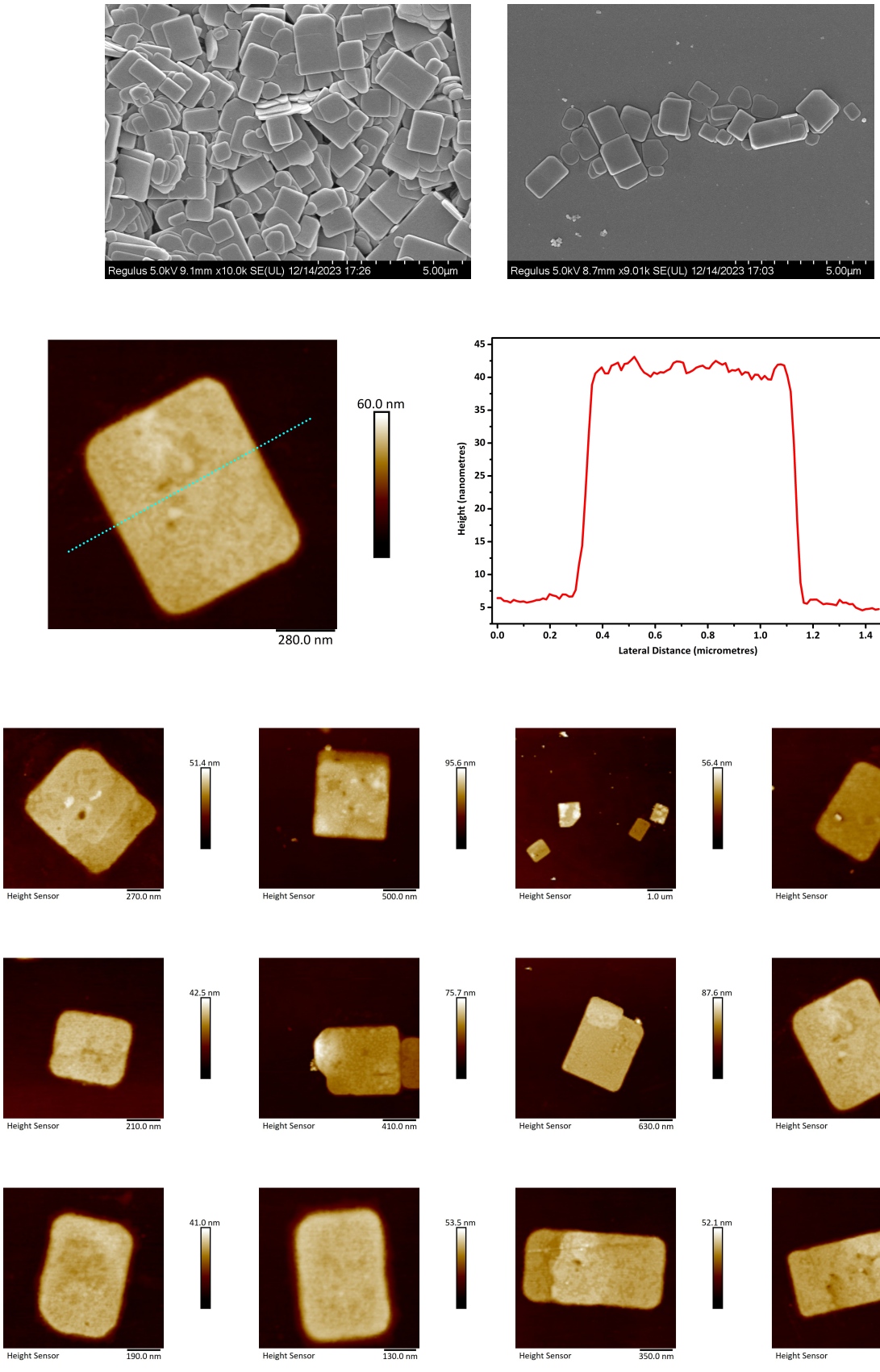

Figure S1. Additional scanning electron microscopy and atomic force microscopy images (with original resolutions of 1320 x 1080 pixels) showing lateral dimensions and thicknesses of $(C_6H_5\text{-}CH_2\text{-}CH_2\text{-}NH_3)_2PbBr_4$ nanoplatelets.

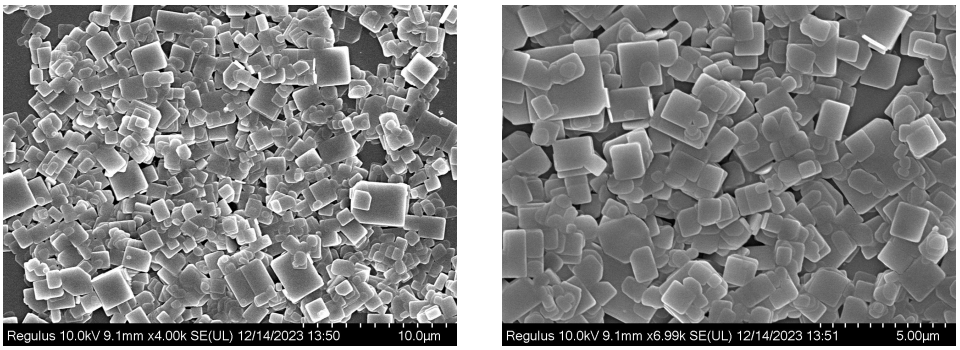

Figure S2. Scanning electron microscopy images showing $(C_6H_5\text{-}CH_2\text{-}CH_2\text{-}NH_3)_2Pb_{0.977}Mn_{0.023}Br_4$ nanoplatelets.

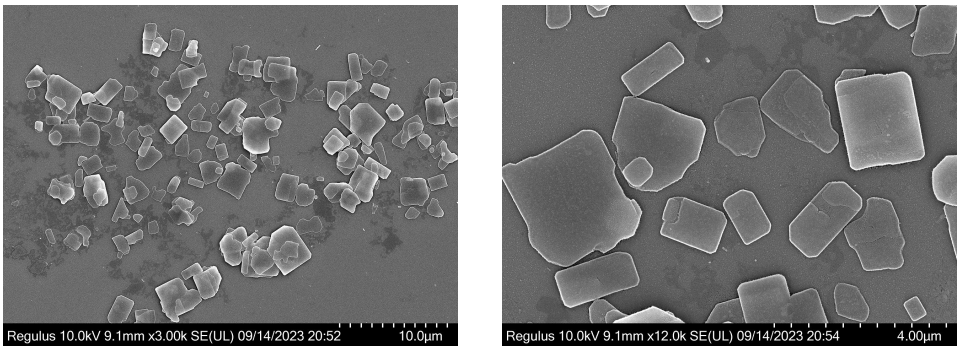

Figure S3. Scanning electron microscopy images showing the geometry of $(C_6H_5\text{-}CH_2\text{-}CH_2\text{-}NH_3)_2PbBr_3I_1$ nanoplatelets.

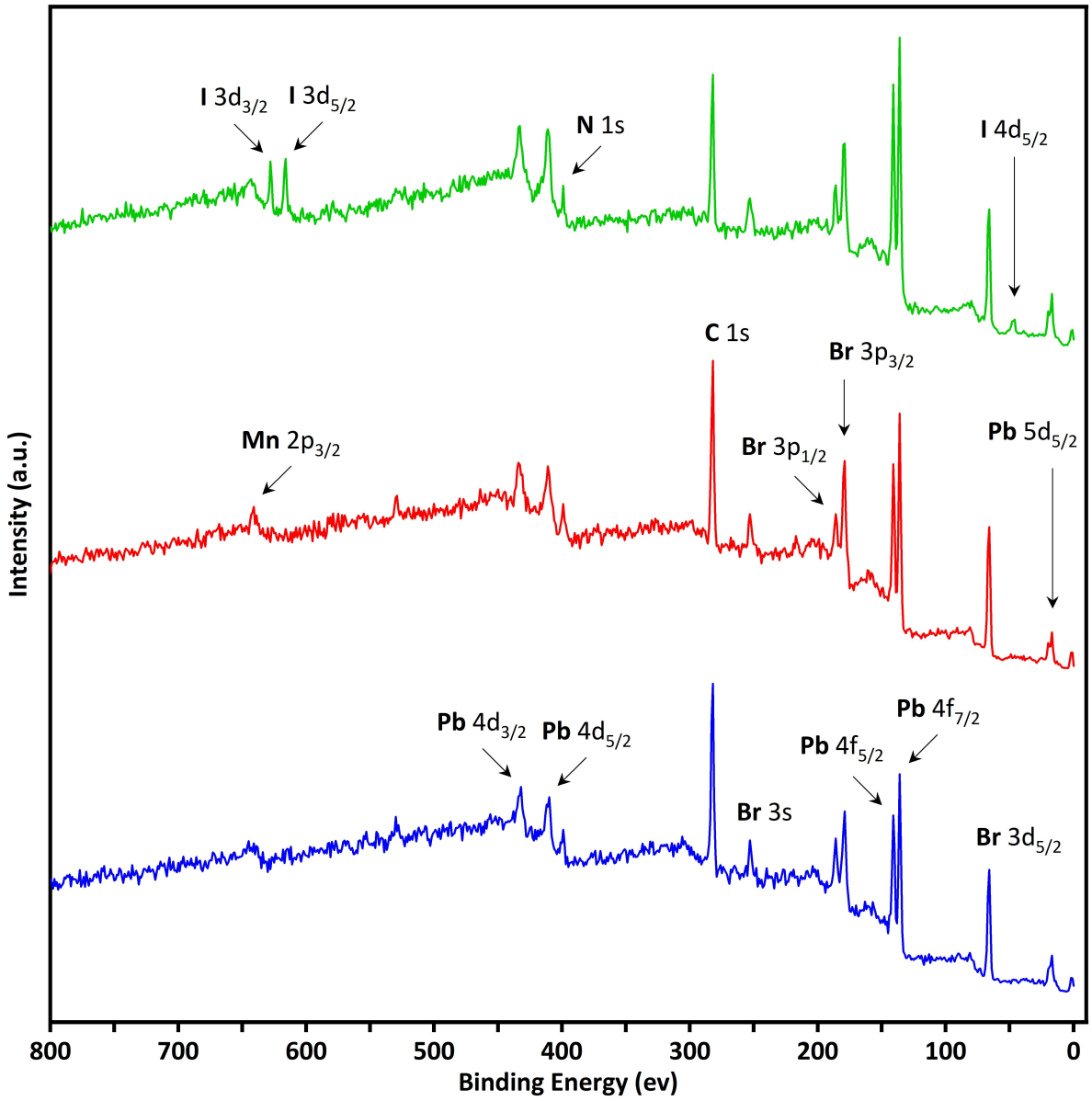

Figure S4. X-ray photoelectron spectroscopy signals of colloidal aerogels of $(C_6H_5\text{-}CH_2\text{-}CH_2\text{-}NH_3)_2PbBr_3I_1$ (upper curve, depicted in green), $(C_6H_5\text{-}CH_2\text{-}CH_2\text{-}NH_3)_2Pb_{0.977}Mn_{0.023}Br_4$ (middle curve, depicted in red), and $(C_6H_5\text{-}CH_2\text{-}CH_2\text{-}NH_3)_2PbBr_4$ (lower curve, blue-colored) perovskite nanoplatelets.

$(C_6H_5\text{-}CH_2\text{-}CH_2\text{-}NH_3)_2Pb_{0.977}Mn_{0.023}Br_4$

BET specific surface area: 4.46 m^2/g

BJH adsorption average pore width: 18.5 nm

$(C_6H_5\text{-}CH_2\text{-}CH_2\text{-}NH_3)_2PbBr_3I_1$

BET specific surface area: 1.87 m^2/g

BJH adsorption average pore width: 9.0 nm

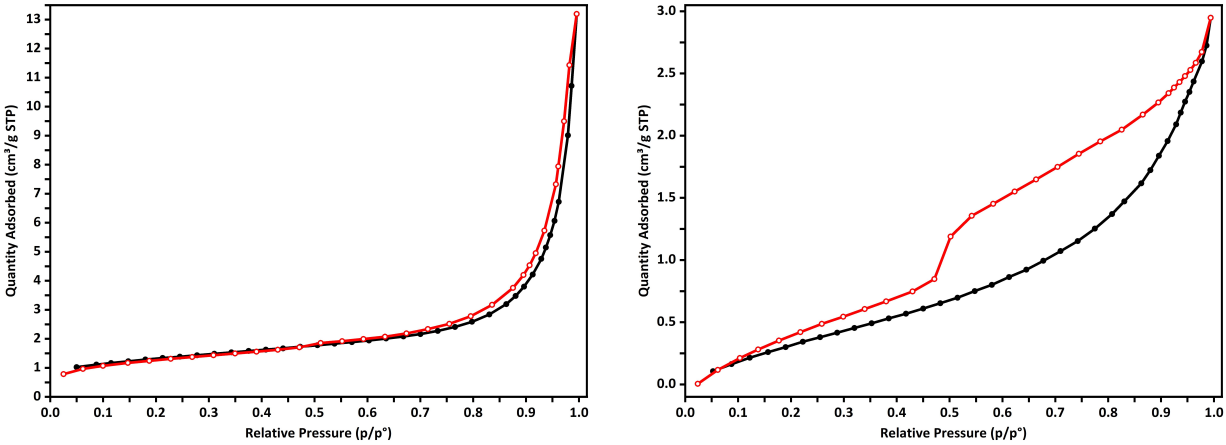

Figure S5. Nitrogen adsorption-desorption isotherms of colloidal aerogels of $(C_6H_5\text{-}CH_2\text{-}CH_2\text{-}NH_3)_2Pb_{0.977}Mn_{0.023}Br_4$ and $(C_6H_5\text{-}CH_2\text{-}CH_2\text{-}NH_3)_2PbBr_3I_1$ perovskite nanoplatelets.

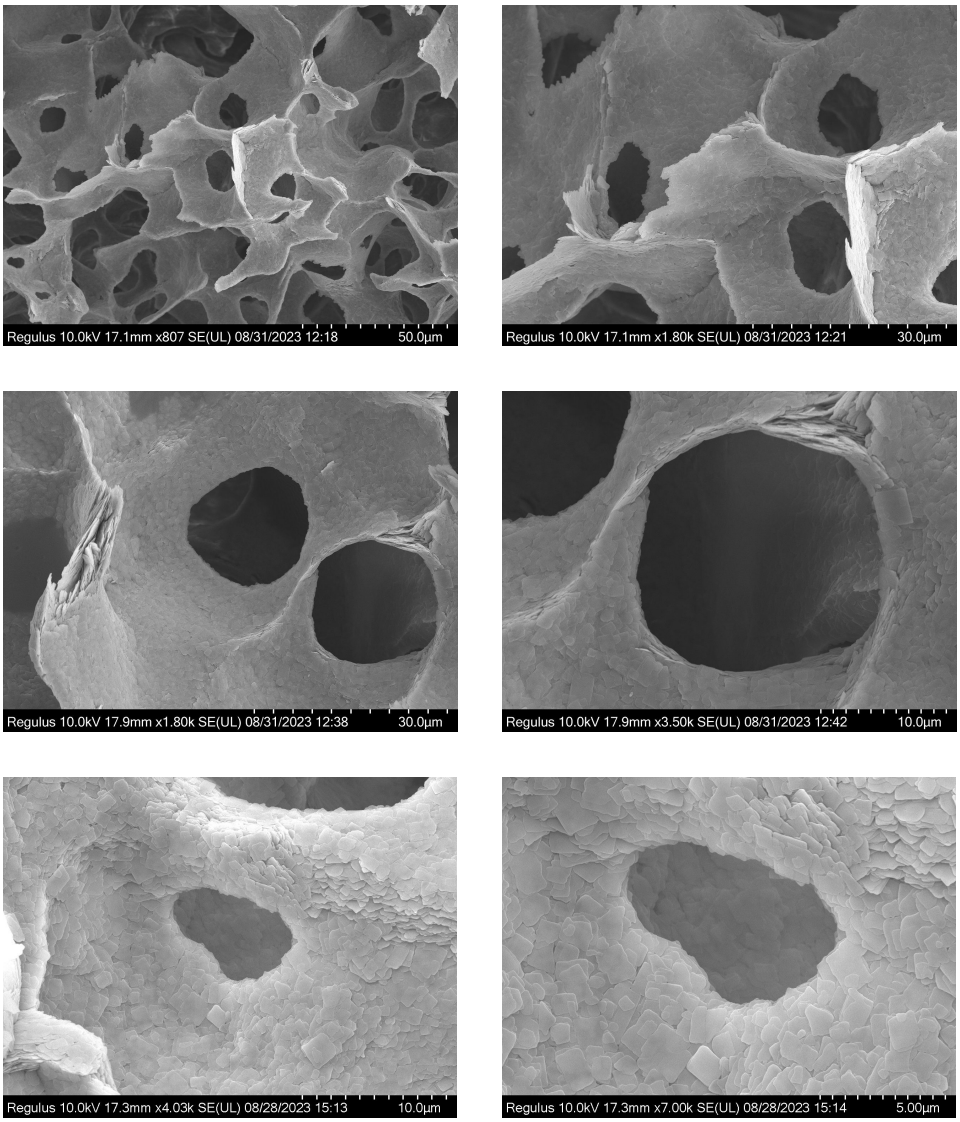

Figure S6. Cross-sectional scanning electron microscopy images of $(C_6H_5\text{-}CH_2\text{-}CH_2\text{-}NH_3)_2PbBr_4$ aerogels.

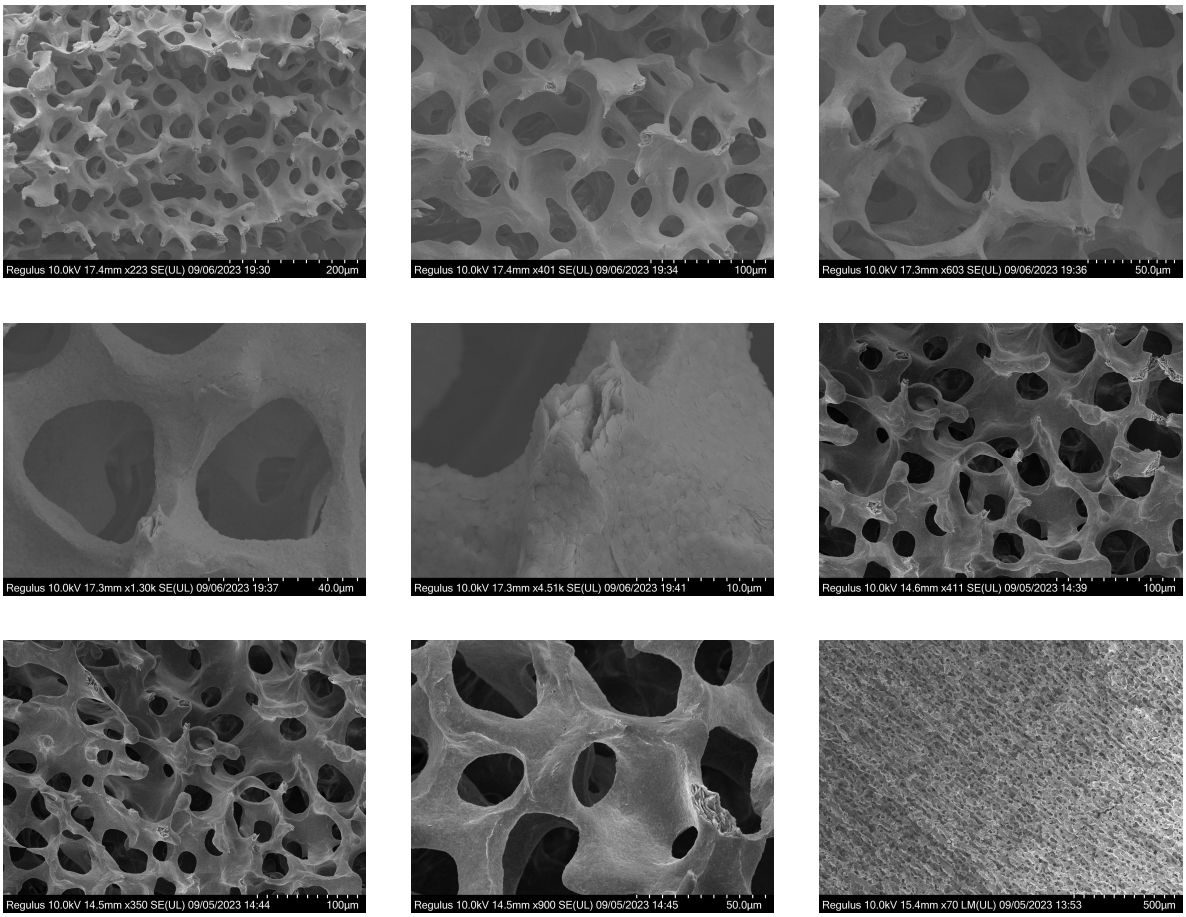

Figure S7. Cross-sectional scanning electron microscopy images of $(C_6H_5\text{-}CH_2\text{-}CH_2\text{-}NH_3)_2Pb_{0.977}Mn_{0.023}Br_4$ aerogels.

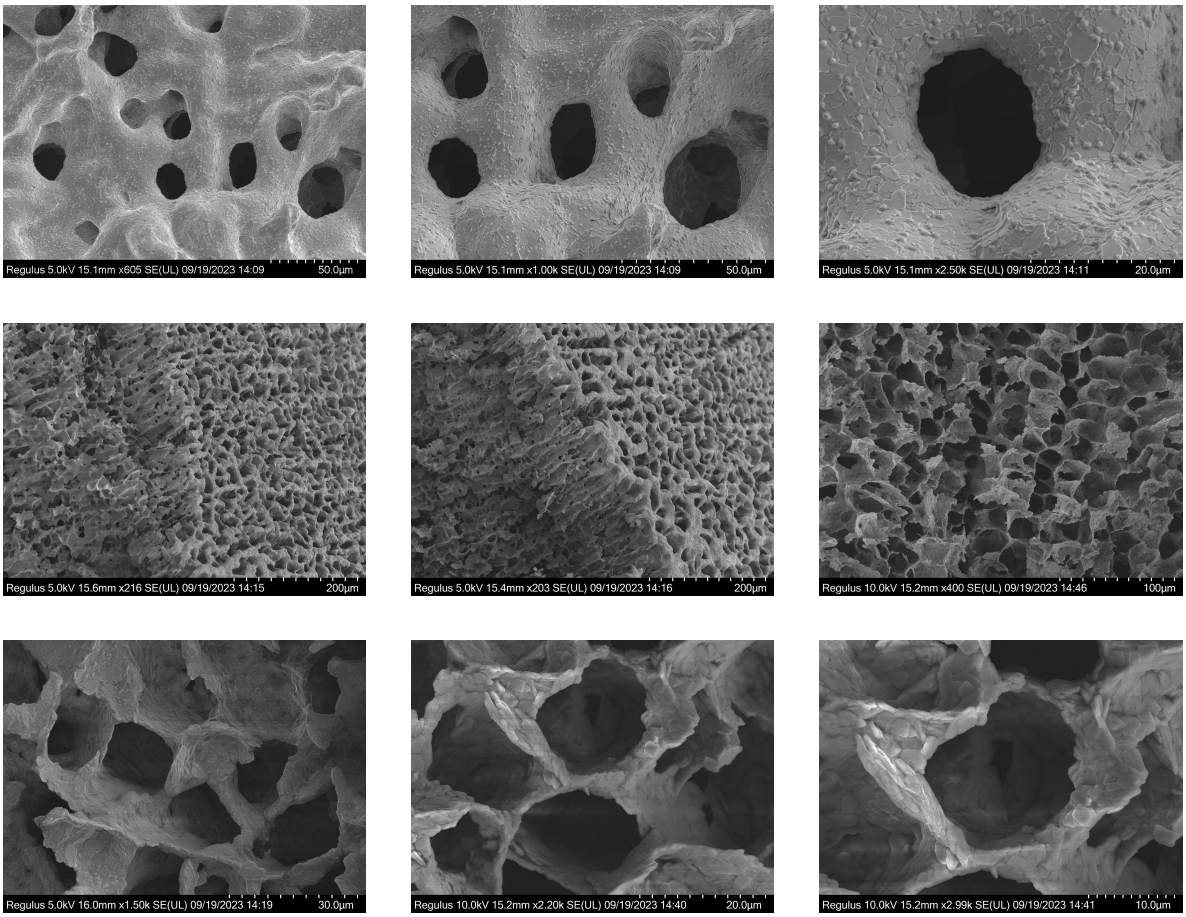

Figure S8. Cross-sectional scanning electron microscopy images of $(C_6H_5\text{-}CH_2\text{-}CH_2\text{-}NH_3)_2PbBr_3I_1$ aerogels.

$(C_6H_5\text{-}CH_2\text{-}CH_2\text{-}NH_3)_2Pb_{0.977}Mn_{0.023}Br_4$

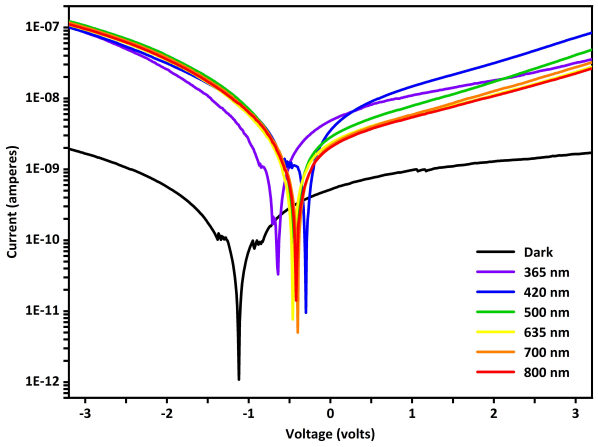

$(C_6H_5\text{-}CH_2\text{-}CH_2\text{-}NH_3)_2PbBr_3I_1$

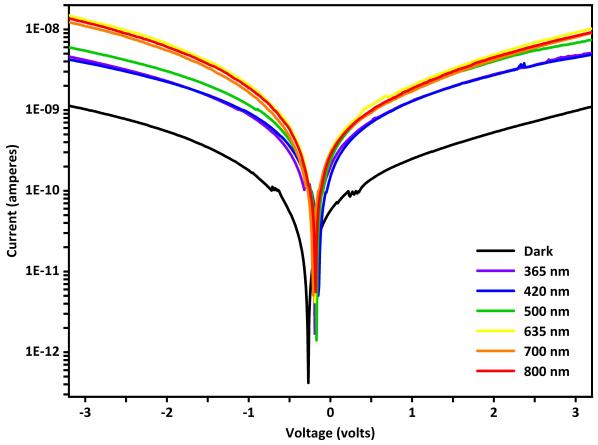

Figure S9. Current-voltage characteristics of $(C_6H_5\text{-}CH_2\text{-}CH_2\text{-}NH_3)_2Pb_{0.977}Mn_{0.023}Br_4$ and $(C_6H_5\text{-}CH_2\text{-}CH_2\text{-}NH_3)_2PbBr_3I_1$ perovskite aerogels under 0.18 mW/mm^2 illumination.

Additional Experimental Methods

Dehydration of chlorobenzene and cyclohexane with copper(II) sulfate anhydrous:

In a 500 mL single-neck round-bottom glass flask, 100 grams of copper sulfate pentahydrate was heated at 523 K for 3 hours until the blue-colored crystals turned grey-white. The flask was closed using a vacuum adapter with a stopcock, then the system was cool down to 298 K. Afterwards, the flask was refilled with dried air to balance the pressure; the vacuum adapter was removed, and 300 mL of chlorobenzene or cyclohexane was immediately injected into the flask to thoroughly mix with copper(II) sulfate anhydrous. The glass flask was then sealed with a rubber stopper so that the dried solvent could be extracted with a syringe.